

Multi-atlas labeling with population-specific template and non-local patch-based label fusion

Vladimir S. FONOV¹, Pierrick Coupé², Simon F. Eskildsen³, Jose Vicente Manjon Herrera⁴, D. Louis Collins¹

¹McConnell Brain Imaging Centre, Montreal Neurological Institute, McGill University, Montreal, Canada. University, 3801 University Street, Montreal, Canada H3A 2B4

²LaBRI UMR CNRS 5800, 33405 Bordeaux, FRANCE

³Center of Functionally Integrative Neuroscience, Aarhus University, Aarhus, Denmark

⁴Instituto de Aplicaciones de las Tecnologías de la Información y de las Comunicaciones Avanzadas (ITACA), Universidad Politécnica de Valencia, Camino de Vera s/n, 46022 Valencia, Spain

Abstract. We propose a new method combining a population-specific non-linear template atlas approach with non-local patch-based structure segmentation for whole brain segmentation into individual structures. This way, we benefit from the efficient intensity-driven segmentation of the non-local means framework and from the global shape constraints imposed by the nonlinear template matching.

Keywords: Non-linear registration, average anatomical template, non-local patch segmentation

1 Introduction

Label fusion segmentation methods have been recently become very popular for solving the automatic structure segmentation problem. Several strategies have been proposed to propagate expert manual segmentations of multiple templates onto a new subject for structure segmentation [1], [2], [3]. In this study, we propose to combine our recently published non-local patch-based segmentation method [4] with population-specific nonlinear template construction [5].

2 Methods

Available anatomical scans from 15 “training” datasets were used to create a left-right symmetric non-linear average anatomical template (see Fig. 1), using the technique described in [5]. Using a left-right symmetric template increases the training library twofold for the patch-based segmentation. The resulting non-linear transformations were applied to the manual segmentations, warping them into a common space forming an anatomical library with twice the number of samples of as in the “training dataset”. Thus, the training library used for the non-local patch-based seg-

mentation algorithm [4] consists of 30 pairs of nonlinearly warped T1w images with their corresponding warped segmentation samples.

2.1 Segmentation method

The procedure segments a new image using the following steps:

1. Image pre-processing includes non-uniformity correction [6], linear intensity normalization using histogram matching between the image and the average template, and affine registration to the template [7].
2. Non-linear registration of the subject's scan to the template [8], using a hierarchical framework, with parameters as described in [5].
3. The scan under study is warped into the template space and the patch-based segmentation algorithm is applied using the anatomical training library (see Fig 1 D,E)
4. The patch-based segmentation is warped back into native scan space using the inverse of the non-linear transformation estimated in step 2.

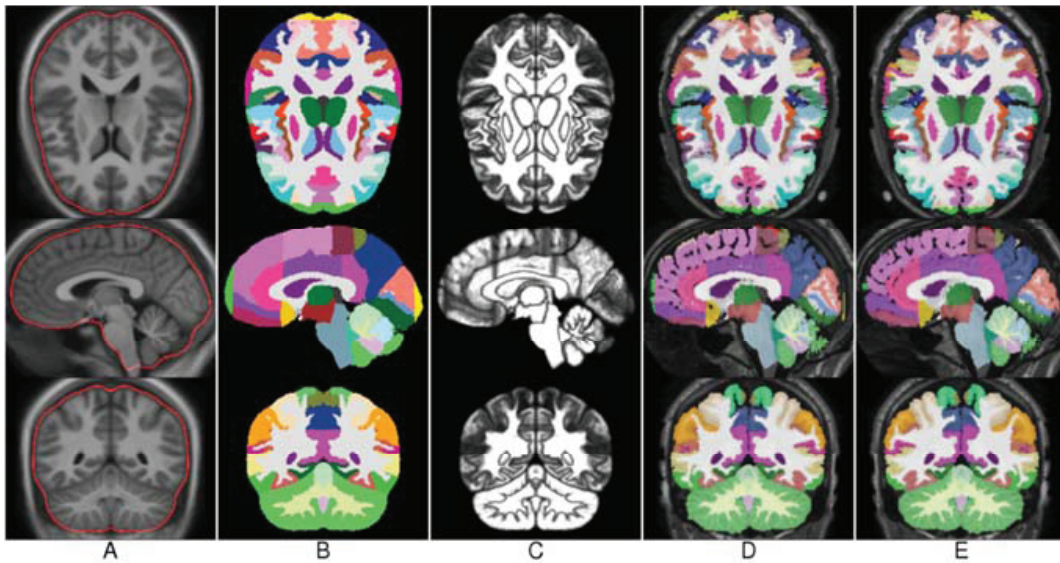


Fig. 1. Average anatomical template, constructed from the training dataset. A: average T1w template; B: majority overlap of anatomical labels for average template; C: pixel-wise generalized overlap, D: example of a one training template in the anatomical library (subject 1000, non-linearly warped into the template space); E: the same template flipped to increase the training library (left-right flipped subject 1000, non-linearly warped into a common space).

2.2 Parameter optimization and validation

The parameters of the non-local patch-based segmentation, i.e., patch size and search area, were chosen using a leave-one-out (LOO) experimental design. For each of the scans from the training dataset, the rest of the available segmentations were used in the algorithm above and the result was compared with the gold standard segmentation provided, using the generalized overlap metric [9].

3 Results

The leave-one-out experiments showed that a patch size of 3x3x3 voxels, and a search area of 7x7x7 voxels provided the best median generalized overlap metric, see see Fig. 2 and Fig. 3. These parameters were then used to segment the “training” dataset.

Average spatial distribution in the errors in LOA experiment is shown on Fig. 4, to produce it each voxel where results of automatic segmentation method disagreed with the ground truth was assigned value of 1, and to 0 otherwise. Resulting binary maps were non-linearly warped into a common space of the template using linear interpolation, and averaged, producing density map of the errors in LOA experiment.

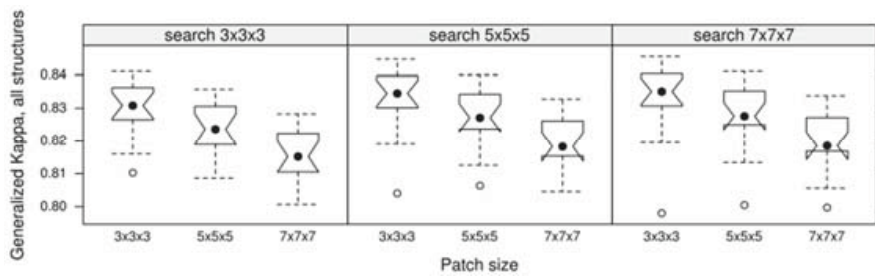


Fig. 2. Results of the leave-one-out experiment, varying parameters of the non-local patch segmentation for all structures.

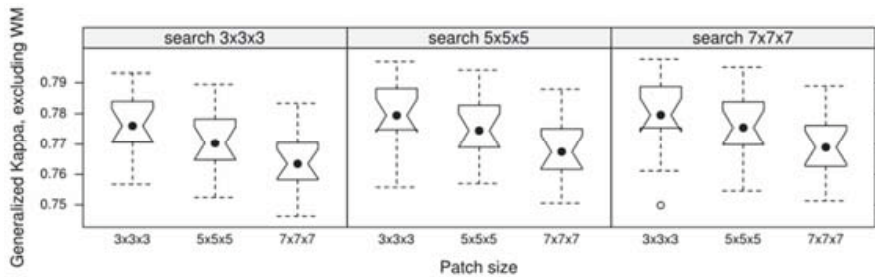


Fig. 3. Results of the leave-one-out for all structures except white matter (excluding IDs 40,41,44,45).

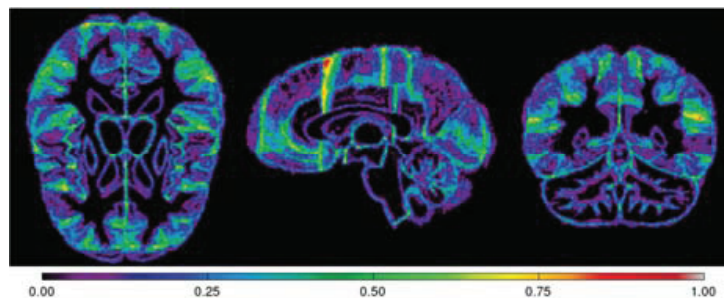


Fig. 4. Spatial distribution of the errors in LOA experiment, 0.00 corresponds to agreement in all cases, 1.00 to a disagreement in all cases.

4 Conclusions

We have created a whole-brain segmentation method which produces promising results in a LOO experiment. It is worth noting that in our LOO experiment the results for the whole brain segmentation may be biased towards structures with relatively large volumes (White Matter of cerebrum and cerebellum), excluding them from analysis reduces generalized overlap ratio (see Fig. 2,3).

The spatial distribution of errors (Fig 4) indicates that majority of segmentation errors occurs on the boundary of two structures, thus overall structures with smaller boundary-to-volume ration are expected to have lower overlap ratio. Furthermore, looking at the Figs. 4, 1C and 1B one can note that the most severe disagreement between automatic segmentation and the ground truth happen on the edge of structures which are defined by a straight line between different elements of the anatomy, not following any visible landmarks.

5 References

1. Aljabar, P., et al., *Multi-atlas based segmentation of brain images: Atlas selection and its effect on accuracy*. NeuroImage, 2009. **46**(3): p. 726-738.
2. Heckemann, R.A., et al., *Automatic anatomical brain MRI segmentation combining label propagation and decision fusion*. NeuroImage, 2006. **33**(1): p. 115-126.
3. Collins, D.L. and J.C. Pruessner, *Towards accurate, automatic segmentation of the hippocampus and amygdala from MRI by augmenting ANIMAL with a template library and label fusion*. NeuroImage, 2010. **52**(4): p. 1355-1366.
4. Coupe, P., et al., *Patch-based segmentation using expert priors: Application to hippocampus and ventricle segmentation*. NeuroImage, 2011. **54**(2): p. 940-954.
5. Fonov, V., et al., *Unbiased average age-appropriate atlases for pediatric studies*. NeuroImage, 2011. **54**(1): p. 313-327.
6. Sled, J.G., A.P. Zijdenbos, and A.C. Evans, *A nonparametric method for automatic correction of intensity nonuniformity in MRI data*. Medical Imaging, IEEE Transactions on, 1998. **17**(1): p. 87-97.
7. Collins, D.L., et al., *Automatic 3D intersubject registration of MR volumetric data in standardized Talairach space*. Journal of Computer Assisted Tomography, 1994. **18**(2): p. 192-205.
8. Collins, D.L., et al., *Automatic 3-D model-based neuroanatomical segmentation*. Human Brain Mapping, 1995. **3**(3): p. 190-208.
9. Crum, W.R., O. Camara, and D.L.G. Hill, *Generalized Overlap Measures for Evaluation and Validation in Medical Image Analysis*. Medical Imaging, IEEE Transactions on, 2006. **25**(11): p. 1451-1461.